

## Electromigration in eutectic SnAg solder reaction couples with various ambient temperatures and current densities

Guang-chen Xu, Fu Guo, and Wan-rong Zhu

College of Materials Science and Engineering, Beijing University of Technology, Beijing 100124, China  
(Received 2008-12-10)

**Abstract:** The electromigration behavior of eutectic SnAg solder reaction couples was studied at various temperature (25 and 120°C) when the current density was held constant at  $10^4$  A/cm<sup>2</sup> or  $5 \times 10^3$  A/cm<sup>2</sup>. Under the current density of  $10^4$  A/cm<sup>2</sup>, scallop type Cu<sub>6</sub>Sn<sub>5</sub> spalls and migrates towards the direction of electron flow at room ambient temperature (25°C), but transforms to layer type Cu<sub>3</sub>Sn and leaves Kirkendall voids in it at high ambient temperature (120°C). Under the current density of  $5 \times 10^3$  A/cm<sup>2</sup> plus room ambient temperature, no obvious directional migration of metal atoms/ions is found. Instead, the thermal stress induced by mismatch of dissimilar materials causes the formation of superficial valley at both interfaces. However, when the ambient temperature increases to 120°C, the mobility of metal atoms/ions is enhanced, and then the grains rotate due to the anisotropic property of β-Sn.

**Key words:** electromigration; eutectic solder; Joule heating; intermetallic compound

[This work was financially supported by the New Century Talent Support Program, Ministry of Education of China (No.NCET-04-0202) and the Beijing Natural Science Foundation Program and Scientific Research Key Program of Beijing Municipal Commission of Education, China (No.KZ200910005004).]

### 1. Introduction

Electromigration (EM) has become a reliability concern to Input/Output (I/O) interconnections in flip chip (FC) packaging and ball grid array (BGA) packaging during recent years. Due to the shrinking size of solder joints, the current density increased dramatically. According to Tu's estimate, EM does occur in FC solder joints at the low current density ( $10^4$  A/cm<sup>2</sup>) which is about two orders of magnitude less than that required to cause EM failure in Al or Cu lines [1-2]. Unlike the single element of Al or Cu lines, solder alloys always contain two more elements. Especially in the solder joints system, there are two interfaces to form intermetallic compound (IMC) layer. Thus, the EM behavior is more complicated to understand. Although the mean-time-to-failure (MTTF) of lead-free solder is longer than that of the lead-containing solder, the morphology evolution of IMC at the interfaces during current stressing represents the polarity effect. Dissolution of IMC at the cathode interface can cause the opening of electrical current path. Accumulation

of IMC at the anode interface can be easily destroyed by exterior stress, such as creep or drop impact, due to the brittleness of IMC by nature.

Eutectic SnAg alloy is one of the prominent lead-free solders to substitute the lead-containing solders. What's more, in order to develop new lead-free solders, eutectic SnAg alloy is usually used as the matrix to accommodate the second phase. Thus, it is necessary to understand the EM behavior of eutectic SnAg alloy. Base on the current knowledge of EM study in eutectic SnAg solder joints, 3 interesting findings can be drawn as follow [3-4]: the failure mode of pancake-type void formation; the fast dissolution of under-bump-metallization (UBM); the non-uniform distribution of current density in solder joints cross-section. However, all these findings might not explain the materials' failure induced by EM. In the geometry of line-to-bump solder joints, electrical current will flow *via* two 90° corners in the solder interconnection which results in obvious current crowding region. The asymmetric constitution of materials in

solder joints can lead to thermal gradient or thermomigration. Multi-coating metal layer on Cu substrate can cause a large gradient of chemical potential energy [5]. All these physical phenomena on solder joints could confuse the researchers to clearly understand the migration of metal atoms/ions propelled by electron wind force. To discover the mechanism of EM-induced failure, a revised structure of solder joints was developed in this paper, which could avoid those un-wanted influences.

## 2. Experimental procedure

Solder reaction couples with a Cu/Sn-3.5Ag/Cu sandwich structure are fabricated to conduct EM study as shown in Fig. 1. Two copper wires in a diameter of 500  $\mu\text{m}$  were first placed into a soldering die with U-grooves, one of which was connected to the translation stage, and then a 500  $\mu\text{m}$  solder ball with Sn-3.5Ag composition and the no-clean flux were both placed into the gap between two copper wires. Finally, the die with the specimen was heated up to 261°C (40°C higher than the melting point of Sn-3.5Ag) and then cooled down to room temperature rapidly by a ventilating fan.

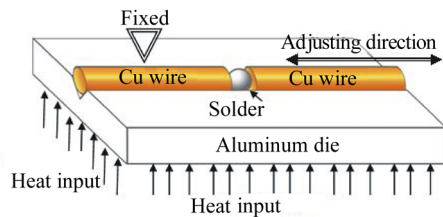


Fig. 1. Soldering set-up for solder reaction couples.

The solder thickness could be precisely controlled through a spiral micrometer in the translation stage. After samples are fabricated, the solder reaction couples are then cold mounted in epoxy resin as shown in Fig. 2.

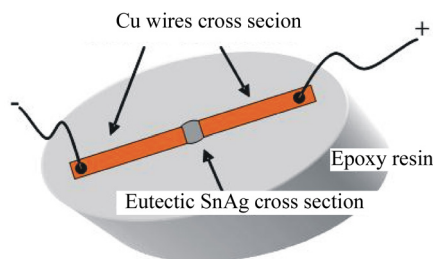


Fig. 2. Cross-sectional area of a specimen after being cold mounted in epoxy resin.

To reach to a high level ( $10^4 \text{ A/cm}^2$  or  $5 \times 10^3 \text{ A/cm}^2$ ) for the current density, half dimension of the specimen was ground and polished to reach a dimension with a cross section of  $1 \times 10^{-3} \text{ cm}^2$ . A current of 10 or 5 A was continuously applied to the specimen; the current

density is  $10^4 \text{ A/cm}^2$  and  $5 \times 10^3 \text{ A/cm}^2$ , respectively. During current stressing, the specimen was exposed to room atmosphere (25°C) or placed into an oven chamber where the temperature was set to 120°C.

## 3. Results and discussion

### 3.1. Joule heating effect at room temperature under various electrical current inputs

The increased surface temperature of the specimen was monitored by a temperature recorder through K-type thermocouples. As shown in Fig. 3, the increased surface temperature of the specimen is mainly from the Joule heating, but the ascending rate of temperature is different with different electrical current inputs (10 and 5 A). When 5 A input is used, the temperature increases rapidly at the beginning 15 min, and then fixes at a constant value of 36°C. However, when 10 A input is used, the temperature increases rapidly at the beginning 30 min, and then fixes at a constant value of 46°C.

Temperature is a key factor to influence the EM behavior of eutectic SnAg solder reaction couples [6-7]. Large electrical current (10 A) input could induce obvious Joule heating effect to solder reaction couples. Accordingly, the mobility of metal atoms/ions was enhanced. Although low electrical current (5 A) input increased the temperature of specimen cross-section, the increased temperature was not high enough to trigger the movement of metal atoms/ions in solder alloys.

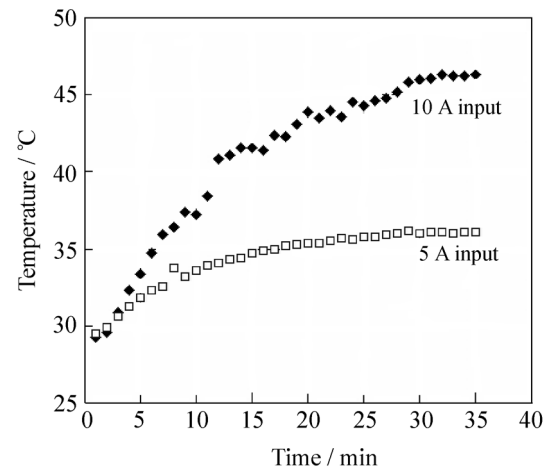


Fig. 3. Temperature profiles of Joule heating effect with electrical current inputs of 5 and 10 A.

### 3.2. Solid state aging at 120°C without current stressing

Solder reaction is the wetting of a molten solder on a solid Cu surface. The wetting reaction forms Cu-Sn IMC at the interface between the molten solder and Cu, and the interface achieves metallic bonding after

cooling, hence two pieces of Cu can be joined by the solder in a solder joint, as shown in Fig. 4. There are 2 IMCs of Cu and Sn:  $\text{Cu}_6\text{Sn}_5$  and  $\text{Cu}_3\text{Sn}$ , and they achieve the wetting reaction as well as the solid-state reactions between Sn and Cu according to the binary phase diagram of Cu-Sn. However, after the first re-flow process, there is no obvious formation of  $\text{Cu}_3\text{Sn}$ , only scallop-type  $\text{Cu}_6\text{Sn}_5$  IMC (less than 5  $\mu\text{m}$  in length) distributes continuously along the interface between solder matrix and Cu substrate. After 7 d of aging process (120°C), the thickness of  $\text{Cu}_3\text{Sn}$  layer increases to 0.783  $\mu\text{m}$ , as shown in Fig. 5.

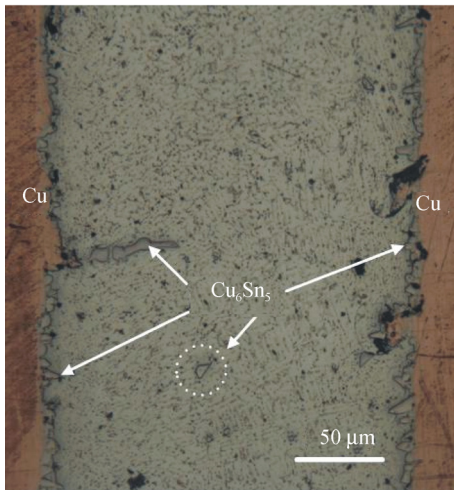


Fig. 4. Specimen cross-section after mechanical grinding and polishing.

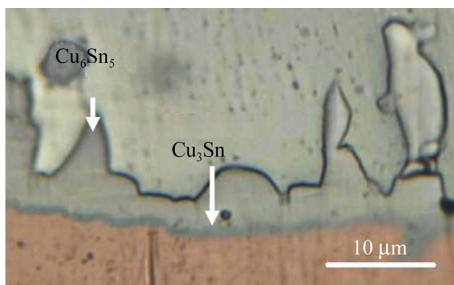


Fig. 5. Interfacial evolution at the interface after 7 d of aging (120°C).

In the classical analysis of solid state interfacial reactions in a binary bulk diffusion couple, it is assumed that all the equilibrium IMCs form simultaneously in a layered morphology. The kinetics of growth of each layer can be diffusion-controlled or interfacial-reaction-controlled. As for the bulk diffusion couple with sufficient thickness and high ambient temperature, all the IMCs coexist and obey a diffusion-controlled growth, so the ratio of thickness among the layers is proportional to the ratio of the square root of the interdiffusion coefficient in each layer [8-9]. The analysis has no consideration of surface and interfacial energies, because the motion of a planar interface in a layered structure does not change energy.

The scallop-type morphology affects the kinetics strongly. The radius of the scallop can not be constant because it must grow bigger with time. If the scallops do not grow in radius, they must grow longer and become a diffusion barrier layer because the valleys will be closed. However, not every scallop can grow in radius, so some of them must shrink. Hence, ripening occurs [10-11]. But the ripening eventually must slow down as the scallops become bigger and bigger. This is because the bigger the scallops, the less the number of short circuit paths (the valleys) to reach the molten solder. In solid-state aging, the rapid gain of free energy disappears, so the compound changes to a layer-type to reduce the interfacial energy [12].

### 3.3. Interior microstructure and surface morphological evolution under $10^4 \text{ A/cm}^2$

As shown in Fig. 6, the growth of IMC at the interfaces exhibits polarity effect after 3 d of current stressing at room ambient temperature. The scallop-type  $\text{Cu}_6\text{Sn}_5$  IMC no longer exists at the cathode interface, rather the IMC has become spheroids and some of them has left the substrate and migrates into the solder matrix by electron wind force, as illustrated in Fig. 7. This might be unexpected because bulk Cu substrate is not consumed by the solder; the interfacial reaction is expected to continue since there is sufficient Cu. Yet electron wind force transforms the hemispherical scallops into spheroids. The transformation from a hemispherical-type scallop to a sphere is driven by the lowering of the sum of surface and interfacial energies in a conservative process.

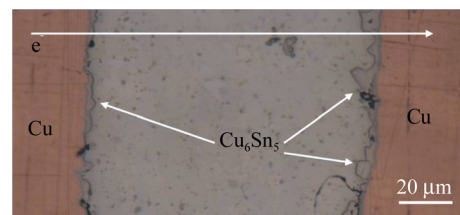


Fig. 6. Interfacial evolution after 3 d of current stressing with the current density of  $10^4 \text{ A/cm}^2$  at room ambient temperature (the symbol e stands for electron wind flow).

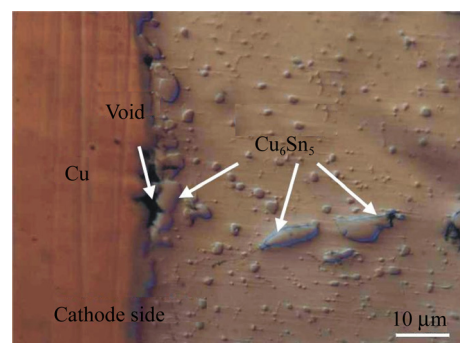


Fig. 7. IMC spalling at the cathode side.

At the anode side, both  $\text{Cu}_3\text{Sn}$  and  $\text{Cu}_6\text{Sn}_5$  layers keep growing with current stressing time and the total thickness approaches to  $10\ \mu\text{m}$  after 3 d, as shown in Fig. 8, comparable to that of thermal aging for 7 d at the same temperature without current application, as shown in Fig. 5. The  $\text{Cu}_3\text{Sn}$  phase between  $\text{Cu}_6\text{Sn}_5$  and Cu has darker color [13-14]. The total IMC at the anode interface is much thicker than that at the cathode interface.

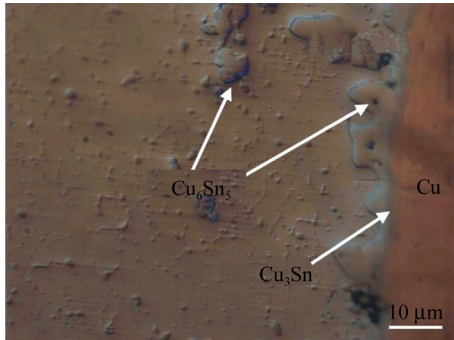


Fig. 8. IMC depositing at the anode side.

With high ambient temperature ( $120^\circ\text{C}$ ), the mobility of metal atoms/ions is enhanced, which means the diffusion rates increases in rising ambient temperature from  $25$  to  $120^\circ\text{C}$ . As shown in Fig. 9, after current stressing for 3 d, the valley is formed near the cathode interface while the extrusion of Sn-Cu IMC layer is formed at the anode interface. When the compressive stress concentrated toward the direction of electron wind flow, the Sn-Cu IMC layer and bulk solder were bulged because the atoms/ions in solder matrix could not diffuse into the Cu substrate at the anode side. Directional migration of atoms/ions induced the formation of tensile stress near the cathode interface. Due to the ductility of solder alloys by nature [15-16], there will be more plastic deformation at the increased ambient temperature. At the maximum tensile stress, some small constrictions or necks begin to form at some point, elongation direction becomes aligned parallel to the direction of electron wind flow, and all subsequent deformation is confined at these necks, as indicated in Fig. 9, and fracture (formation of the valley) ultimately occurs at these necks.

To examine the interior microstructure at the anode interface, the fluctuation of specimen cross-section was ground and polished again. As shown in Fig. 10, IMC formation at the anode interface is occupied by the growth of  $\text{Cu}_3\text{Sn}$  instead of  $\text{Cu}_6\text{Sn}_5$ . The formation of  $\text{Cu}_3\text{Sn}$  is accompanied by the formation of a large number of Kirkendall voids in the layer and especially in the interface between  $\text{Cu}_3\text{Sn}$  and solder matrix. The competition in growth between  $\text{Cu}_6\text{Sn}_5$  and  $\text{Cu}_3\text{Sn}$  tended to favor the latter when the ratio of Cu to Sn

was large in the solder matrix. The transformation of 1 molecule of  $\text{Cu}_6\text{Sn}_5$  into 2 molecules of  $\text{Cu}_3\text{Sn}$  left behind 3 Sn atoms, which attracted 9 atoms of Cu to form 3 more molecules of  $\text{Cu}_3\text{Sn}$  [17]. The vacancy flux needed to transport Cu atoms accumulated at the solder matrix/ $\text{Cu}_3\text{Sn}$  interface to form Kirkendall voids. The growth of  $\text{Cu}_3\text{Sn}$  was not only controlled by time, temperature, impurities, and the ratio of Cu/Sn, but also by external forces, such as EM.

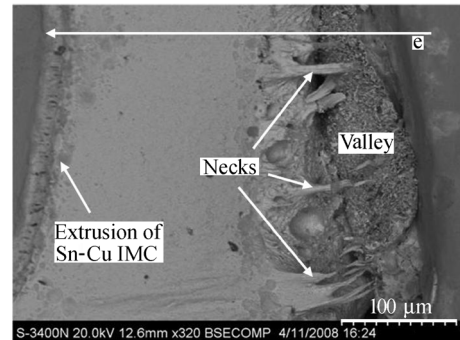


Fig. 9. Morphology evolution after current stressing for 3 d under the current density of  $10^4\ \text{A}/\text{cm}^2$  at the ambient temperature of  $120^\circ\text{C}$ .

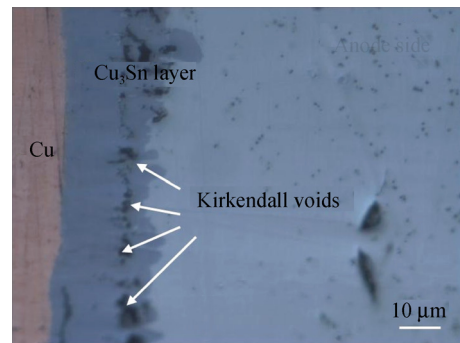


Fig. 10. Interior microstructure of the anode interface.

### 3.4. Interior microstructure and surface morphological evolution under $5 \times 10^3\ \text{A}/\text{cm}^2$

When the specimen was subjected the current density of  $5 \times 10^3\ \text{A}/\text{cm}^2$  plus low ambient temperature ( $25^\circ\text{C}$ ), the morphological IMC has unchanged both at the anode interface and the cathode interface, because the lower activation energy of diffusion entity. At high ambient temperature ( $120^\circ\text{C}$ ), the growth of IMC at the interface during current stressing has changed from scallop-type to layer-type at the cathode interface as shown in Fig. 11(a), but the scallop-type IMC at the anode interface has unchanged during current stressing for 3 d as shown in Fig. 11(b). The growth of IMC was retarded by low diffusion rate of Cu atoms from substrate to solder matrix under low current density. Thus, the scallop-type of  $\text{Cu}_6\text{Sn}_5$  remained the same at the anode interface.

Before the current stressing, the specimen cross-section is flatness. However, after current stressing for

3 d, a superficial valley appears both at the anode interface and the cathode interface, as illustrated in Fig. 12. The volume of the solder alloy between two Cu substrates was constant, and the IMC at the interface and Cu substrate acted as rigid walls to prevent plastic deformation of the solder alloy. Accordingly, the plastic deformation of the solder alloy could only occur at the vertical direction of electron wind flow. To reduce the interfacial and surface energies of the solder alloy at the constant volume, two superficial valleys formed at the both interface.

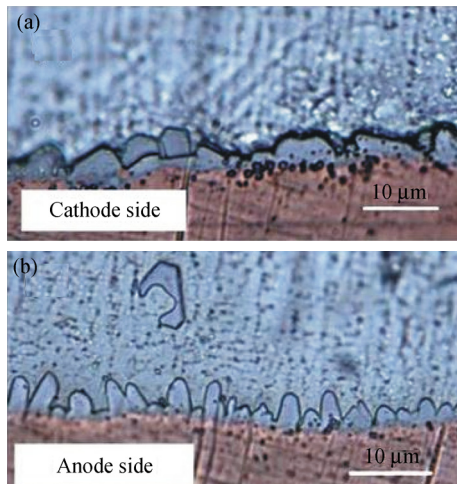


Fig. 11. Growth of IMC at the interface after current stressing for 3 d under the current density of  $5 \times 10^3$  A/cm<sup>2</sup> plus 120°C: (a) cathode interface; (b) anode interface.

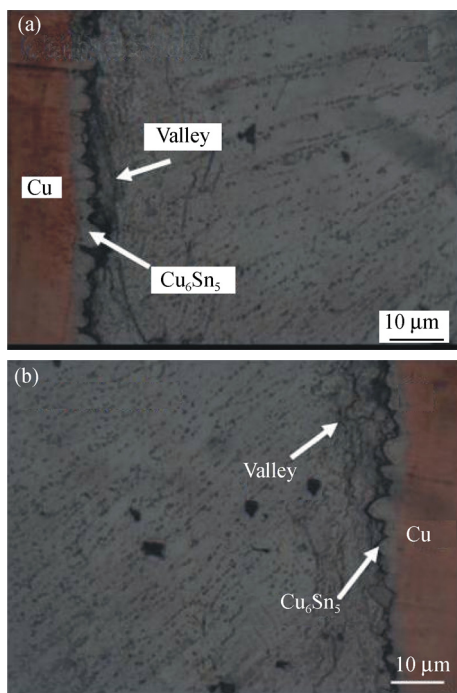


Fig. 12. Interfacial evolution after current stressing for 3 d under the current density of  $5 \times 10^3$  A/cm<sup>2</sup> at room ambient temperature: (a) cathode side; (b) anode side.

In the eutectic SnAg alloy, some very large platelet-type Ag<sub>3</sub>Sn IMC can be seen, as illustrated in Fig.

13(a). During plastic deformation induced by compressive stress of metal atoms/ions accumulation, the crystallographic lattice of individual grains rotated, giving rise to an evolution of deformation textures at the bulk level. Due to the long hours of current stressing, the deformation of β-Sn grains occurs at the free surface of solder reaction couples, as shown in Fig. 13(b). It appeared that β-Sn grains present in this region experienced grain boundary (GB) sliding due to current stressing. Such GB sliding was not observed in the interior regions of the solder reaction couples although it was pronounced in regions near the free surface of the solder reaction couples. Fig. 14 reveals that similar GB sliding occurs in regions around the major

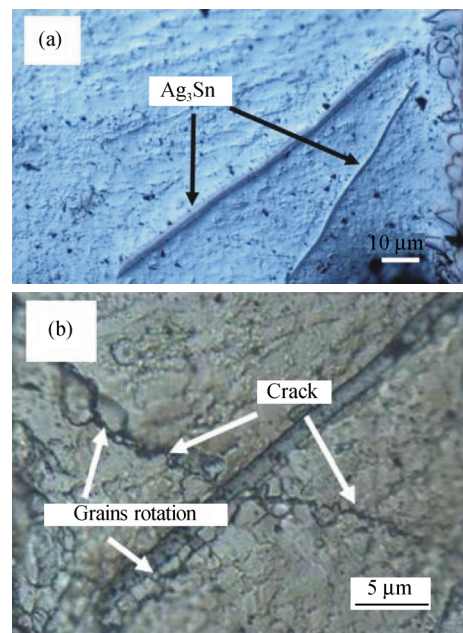


Fig. 13. Microstructure evolution of Ag<sub>3</sub>Sn under the current density of  $5 \times 10^3$  A/cm<sup>2</sup> plus 120°C: (a) without current stressing; (b) current stressing after 3 d.

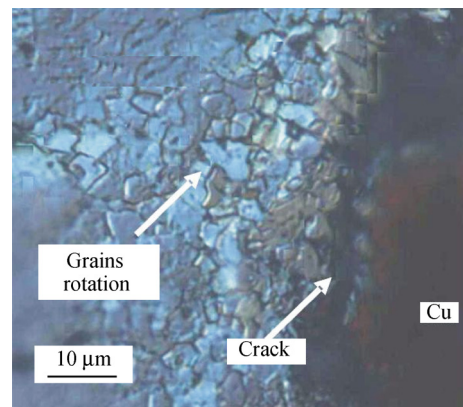


Fig. 14. Microstructure evolution at the anode side under the current density of  $5 \times 10^3$  A/cm<sup>2</sup> plus 120°C.

crack. This indicates that GB sliding is accompanied by the formation and propagation of the crack propagated through regions in the bulk solder near the Cu substrate. Thus, under the stress state used, slip would

cause material to move into the surface, as suggested by the split unit, but the constraint by the substrates prevented free rotation of the crystal. Therefore, discontinuous shear that allowed the crystal to rotate while constrained could account for the ledges [18-19].

#### 4. Conclusions

(1) Different electrical current inputs can induce the different Joule heating effect. The surface temperature of solder reaction couples increases from 25 to 36°C when 5 A is applied. However, when 10 A is applied, the surface temperature can reach to 46°C. Thus, the more the electrical current input, the more the Joule heating effect can be generated.

(2) Only scallop-type Cu<sub>6</sub>Sn<sub>5</sub> IMC distributes continuously along the interface between solder matrix and Cu substrate after solidification. Without current stressing, Cu<sub>3</sub>Sn appears at both interfaces after 7 d of aging process (120°C).

(3) Under high current density (10<sup>4</sup> A/cm<sup>2</sup>), mass movement is obvious even at room temperature, IMCs at the cathode interface can spall and migrate to the anode side. The directional movement of IMCs eventually deposits at the anode interface, which became much thicker than the cathode interface. However, at high ambient temperature (120°C), the chemical reaction at the interface is enhanced, Cu<sub>6</sub>Sn<sub>5</sub> transforms to Cu<sub>3</sub>Sn which induces the appearance of Kirkendall voids at the tip of Cu<sub>3</sub>Sn layer next to solder matrix.

(4) Under low current density (5×10<sup>3</sup> A/cm<sup>2</sup>), mass movement is retarded due to the lower activation energy. At room temperature, the thermal stress induced by mismatch of dissimilar materials can cause a superficial valley at both interfaces. However, at high ambient temperature (120°C), the mobility of grains is enhanced which can cause the rotation of β-Sn.

#### References

- [1] K.N. Tu, Electromigration in stressed thin films, *Phys. Rev. B*, 45(1992), No.3, p.1409.
- [2] K.N. Tu, Recent advances on electromigration in very-large-scale-integration of interconnects, *J. Appl. Phys.*, 94(2003), No.9, p.5451.
- [3] L. Zhang, S. Ou, J. Huang, K.N. Tu, S. Gee, and L. Nguyen, Effect of current crowding on void propagation at the interface between intermetallic compound and solder in flip chip solder joints, *Appl. Phys. Lett.*, 88(2006), art. no.012106.
- [4] S.W. Chen, S.K. Lin, and J.M. Jao, Electromigration effects upon interfacial reactions in flip-chip solder joints, *Mater. Trans.*, 45(2004), p.661.
- [5] C.E. Ho, A. Lee, and K.N. Subramanian, Design of solder joints for fundamental studies on the effects of electromigration, *J. Mater. Sci. Mater. Electron.*, 18(2007), p.569.
- [6] H.T. Orchard and A.L. Greer, Electromigration effects on compound growth at interfaces, *Appl. Phys. Lett.*, 86(2005), art. no.231906.
- [7] C. Chen and S.W. Liang, Electromigration issues in lead-free solder joints, *J. Mater. Sci. Mater. Electron.*, 18(2007), p.259.
- [8] U. Gosele and K.N. Tu, Growth kinetics of planar binary diffusion couples: Thin film case versus bulk cases, *J. Appl. Phys.*, 53(1982), p.3252.
- [9] K.N. Tu, F. Ku, and T.Y. Lee, Morphological stability of solder reaction products in flip chip technology, *J. Electron. Mater.*, 30(2001), No.9, p.1129.
- [10] J. Gorlich, G. Schmidt, and K.N. Tu, On the mechanism of the binary Cu/Sn solder reaction, *Appl. Phys. Lett.*, 86(2005), art. no.053106-1.
- [11] A.A. Liu, H.K. Kim, K.N. Tu, *et al.*, Spalling of Cu<sub>6</sub>Sn<sub>5</sub> spheroids in the soldering reaction of eutectic SnPb on Cr/Cu/Au thin films, *J. Appl. Phys.*, 80(1996), p.2774.
- [12] A.M. Gusak and K.N. Tu, Kinetic theory of flux driven ripening, *Phys. Rev. B*, 66(2002), p.115403.
- [13] H. Gan and K.N. Tu, Polarity effect of electromigration on kinetics of intermetallic compound formation in Pb-free solder V-groove samples, *J. Appl. Phys.*, 97(2005), art. no.063514-1.
- [14] H. Gan, W.J. Choi, G. Xu, and K.N. Tu, Electromigration in flip chip solder joints and solder lines, *JOM*, 6(2002), p.34.
- [15] F. Ren, J.W. Nah, K.N. Tu, *et al.*, Electromigration induced ductile-to-brittle transition in lead-free solder joints, *Appl. Phys. Lett.*, 89(2006), art. no.141914.
- [16] J.W. Nah, F. Ren, K.W. Paik, *et al.*, Effect of electromigration on mechanical shear behavior of flip chip solder joints, *J. Mater. Res.*, 21(2006), No.3, p.698.
- [17] T.Y. Lee, W.J. Choi, K.N. Tu, *et al.*, Morphology, kinetics and thermodynamics of solid state aging of eutectic SnPb and Pb-free solders (SnAg, SnAgCu, and SnCu) on Cu, *J. Mater. Res.*, 17(2002), No.2, p.291.
- [18] N. Bernstein, The influence of geometry on grain boundary motion and rotation, *Acta Mater.*, 56(2008), p.1106.
- [19] G. Winther, Slip systems, lattice rotations and dislocation boundaries, *Mater. Sci. Eng. A*, 40(2008), p. 483.